Molecular-orbital description of the states of two-electron systems

James M. Feagin
Department of Physics, California State University, Fullerton, California 92634

John S. Briggs
Fakultät für Physik, Universität Freiburg, D-7800 Freiburg, West Germany
(Received 20 January 1988)

The molecular-orbital (MO) method introduced previously by us [Phys. Rev. Lett. **57**, 984 (1986)] to treat two-electron atoms is developed further. The states of systems consisting of two electrons and one positively charged particle are analyzed with use of the interelectronic distance as an adiabatic coordinate in analogy to the interprotonic distance in H_2^+. The motion of two electrons then separates into rotational, vibrational, and internal motion, the latter being described by MO, exactly as in molecules. Indeed, adiabatic MO potential curves for atomic systems are obtained by scaling the corresponding curves for H_2^+. Approximate quantum numbers for two-electron states, derived previously by empirical methods or from an *ad hoc* rovibrational model, arise naturally since the two-center Coulomb problem is exactly separable in MO coordinates and the corresponding nodal surfaces are conserved for all interelectronic separations. In addition, the *gerade-ungerade* symmetry of MO is exactly preserved and appears as a fundamental symmetry of two-electron states.

I. INTRODUCTION

The three-body Coulomb system of two electrons and one positively charged particle (e.g., He,H^-,Ps^-) is the fundamental testing ground for the description of electron correlations. This is because, in doubly excited states of helium or in all states of H^-, the electron-electron interaction is of equal importance to the electron-ion interaction. This correlation effect becomes more and more pronounced as the energy of the three-body system approaches that for complete fragmentation.[1]

The earliest and still numerically most effective method by which to describe two-electron correlated states is to represent them as linear superpositions of products of one-electron atomic states. By inclusion of a sufficient number of terms of a given symmetry, high accuracy in the positions of resonances can be obtained as exemplified by the calculations of Lipsky *et al.*[2] on helium autoionizing states. This method suffers from the obvious drawback that, apart from examining the relative contributions of different one-electron orbital products or plotting out the wave function itself, there is no systematic way in which the character of the two-electron motion can be classified and hence understood in simple terms. Nevertheless, in certain cases, specific linear combinations of one-electron product states do have a large-enough weight to allow a simple approximate classification. The best example of this is the "+" and "−" classification used by Cooper *et al.*[3] to describe series of autoionizing states of the helium atom.

A significant advance in the understanding of correlated two-electron motion has resulted from the use of hyperspherical coordinates, first exploited in this connection by Macek.[4] For example, Macek gave an alternative description of the + and − series of states by interpreting them as series of "vibrational" states based upon two potential wells of quite different character with respect to adiabatic variation of the hyperspherical radius $\mathcal{R}=(r_1^2+r_2^2)^{1/2}$, where $\mathbf{r}_1$ and $\mathbf{r}_2$ are the positions of the electrons with respect to the nucleus. This *adiabatic* hyperspherical approximation has since been extensively employed[1] to discuss not only the helium atom[5–7] but also the ground and resonant states of H^- [Ref. 5(b)] and Ps^- (Ref. 8), the negative ions of hydrogen and positronium. The success of the method in the qualitative explanation of correlated motion in terms of the variation of hyperspherical coordinates describing radial and angular electron correlation is impressive. Again, however, only states of total symmetry are identified by the separation of the two-electron problem in hyperspherical coordinates, and no approximate "internal" quantum numbers arise naturally in the method.

The identification of a new scheme of quantum numbers with which to classify correlated motion of two electrons is the core of the problem and has occupied much effort over the last ten years. Herrick and co-workers[9–11] approached the problem from the opposite end, by first assuming certain symmetry properties and then considering to what extent the observed energy levels fitted into this scheme. Since the one-electron orbitals of hydrogenic atoms form a representation of the group O(4), with angular momentum l and Runge-Lenz vector $\mathbf{a}$ as conserved quantities, they considered decompositions of the product group $[O(4)]_1\times[O(4)]_2$ for the two electrons with generators $\mathbf{L}=\mathbf{l}_1+\mathbf{l}_2$ and $\mathbf{A}=\mathbf{a}_1-\mathbf{a}_2$. In particular, they identified a quantum number T associated with the projection of $\mathbf{L}$ along an internal axis $\hat{\mathbf{A}}$ and a further quantum number K_H depending upon T and the principal quantum number of the one-electron shell involved. (Herrick used the label K for this quantum number. We will use the notation K_H to avoid confusion with the

molecular angular momentum projection quantum number K to be introduced later.) The occurrence of the angular momentum projection quantum number T led Herrick and Kellman[12] to suggest that a corresponding term proportional to $[L(L+1)-T^2]$, a rotor energy term, may describe the energy-level spectra. Since such a two-electron atom as rotor would not be rigid, they further surmised that a bending vibrational degree of freedom would also be present, giving rise, in essence, to a rovibrational spectrum analogous to that observed for a triatomic XYX molecule. We will return to this model later.

Lin[5(c)] adopted a more pragmatic approach and simply made relief plots of the adiabatic wave functions in hyperspherical coordinates. By inspection of the wavefunction character with respect to the hyperspherical angle $\alpha=\tan^{-1}(r_1/r_2)$, he was able to classify the wave functions according to three types of behavior, for which he introduced the quantum number, or strictly speaking the label, A with values $+$, $-$, or 0. In a further paper, Lin[5(a)] was able to classify sequences of helium-doubly-excited states according to the quantum numbers K_H, T, and A.

The hyperspherical coordinates have also been used with considerable success to discuss the three-body Coulomb breakup leading to the "Wannier mode" at threshold (see Ref. 1 for a discussion of this work). The use of molecular coordinates, as in the H_2^+ problem, was also suggested for the discussion of the two-electron, one-nucleus problem.[13] In this application, the molecular internuclear axis $\mathbf{R}$ is replaced by the interelectronic axis $\mathbf{R}=\mathbf{r}_1-\mathbf{r}_2$, and the H_2^+ electronic coordinate $\mathbf{r}$ is replaced by the position of the nucleus with respect to the center of mass (c.m.) of the two electrons. In these explicitly molecular coordinates, a detailed analysis of the Wannier problem was given.[13(a)] Prompted by this success, the molecular-orbital (MO) model was applied[13(b),14] to a discussion of the resonant states of helium, H^-, and Ps^- converging to the $N=2$ one-electron level. It was shown that adiabatic molecular-orbital potential curves as functions of R show a remarkable similarity to the hyperspherical ones but have the advantage that well-defined internal quantum numbers are assigned to them. Moreover, having recognized the analogy between two-electron atoms and H_2^+, the rovibrational structure follows immediately, as in the molecular case. In the atom, however, it is the projection of the total angular momentum along the interelectronic axis that is a quantum number. The vibrational part is simply the "breathing" motion of the coordinate R. In the MO model, as shown in Sec. II, the remaining two degrees of freedom are those used to separate the MO problem and both have an associated quantum number. We emphasize the fundamental difference between the MO model and the rovibrational model introduced by Herrick and Kellman,[12] enlarged upon by Berry and co-workers,[15–17] and compared to the hyperspherical results by Watanabe and Lin.[18] In the latter model, the molecular analog of a two-electron atom is taken to be a linear triatomic molecular with no *electronic* degrees of freedom. The breathing and bending vibrations and their associated wave functions are introduced in an *ad hoc* manner. In our case, the "molecule" possesses the rotational, vibrational, and electronic degrees of freedom arising naturally from the coordinate separation, and all corresponding wave functions can be derived in a well-defined way. The rotational part is common to both; indeed, although discussing Herrick's triatomic model, Watanabe and Lin used the MO-model rotation with $\hat{\mathbf{R}}$ as quantization axis and showed the relationship to Herrick's use of $\hat{\mathbf{A}}$.

In a previous paper [Ref. 14(b), hereafter referred to as I], we showed that the T quantum number is nothing more than the σ, π, δ, etc. quantum number characterizing the diatomic, or in this case "dielectronic" MO. Here we will discuss the symmetries of the MO model further. In particular, it will be shown that Herrick's quantum number K_H is equal to (n_2-n_1) where n_1,n_2 are the parabolic quantum numbers of the separated-atom (SA) state to which the MO correlates. Furthermore, we will show that Lin's label A is given by $(-1)^{n_\mu}$ and n_μ is the MO quantum number corresponding to the coordinate $\mu=(r_1-r_2)/R$.

A further, more fundamental symmetry with which to characterize two-electron states will emerge. This is the *gerade-ungerade (g-u)* symmetry of the adiabatic MO. This "internal" symmetry is not broken by any of the off-diagonal couplings that are neglected in the molecular separation and remains a symmetry of the total state of the two-electron atom. Indeed, if g symmetry is denoted by $+1$ and u symmetry by -1, then this MO quantum number is given by the product $\pi(-1)^S$, where π is the parity and S the spin of the two-electron atom state. Hence the grouping of certain sequences of states, e.g., ${}^1S^e$, ${}^3P^o$,${}^1D^e$, etc., which have been observed, is explained by their being based on a single MO of given g character, since $\pi(-1)^S=+1$ for this sequence. Therefore, we suggest that the labeling of two-electron states by spin S and g (even) or u (odd) character may be more useful than the usual labeling by spin- and total-parity π, since the latter quantum number has no particular significance for electron correlation.

The further advantage of the MO model, discussed in I and to be described in more detail here, is the scaling property of the adiabatic MO potential curves. This property enables us to derive potential curves for the three systems He, H^-, and Ps^- with a minimum of calculation, simply by scaling the published curves for the H_2^+ molecule. In fact, the MO model of two-electron atoms and the scaling property were introduced over 20 years ago by Hunter and co-workers.[19,20] Unfortunately, these authors did not describe the general construction of eigenstates of given total angular momentum and parity and restricted discussion to the ground and singly excited states. In these states, the electron correlation is not dominant, and the MO model gives only a moderate estimate of binding energies. Probably for this reason, the method was not pursued further. Nevertheless, we find it instructive to consider the way in which the MO model correctly predicts the qualitative nature of the low-lying spectra of all the three-body Coulomb systems H_2^+, He, H^-, and Ps^-. In particular, one sees how the relevant mass and charge ratios influence the nature of the spectra.

In the four systems H_2^+, He, H^-, and Ps^-, the lowest state is one of zero total angular momentum based on the lowest orbital of σ type. Since all systems contain two identical particles, the MO have the g or u symmetry with respect to the midpoint of the line joining these two particles. Hence, as is well-known for H_2^+, the two lowest-potential curves are those based on the $1s\sigma_g$ and $2p\sigma_u$ MO, as shown in Fig. 1 schematically for all four cases. For H_2^+, the $1s\sigma_g$ MO is a bonding orbital, and there is a potential well supporting the bound states, the lowest of which is the zero angular momentum rotationless and vibrationless $^2\Sigma_g$ state. The center of mass of the molecule is practically at the midpoint of the nuclei, and the reduced mass and momenta of inertia of the nuclear motion are proportional to the nuclear mass. This gives vibrational and rotational energy spacings that are very small compared to the electronic well depth, so that H_2^+ possesses a rich rovibrational spectrum based on the $1s\sigma_g$ MO. The $2p\sigma_u$ is an antibonding MO and gives a fully repulsive $^2\Sigma_u$ curve as $R \to \infty$, i.e., as one proton moves off. Hence there are no bound states based on the $2p\sigma_u$ MO.

The system H^- is similar to H_2^+ in that, again, all three charges are of the same magnitude and one mass ratio is unity, while the others involve the ratio of proton to electron mass. As shown in Fig. 1, the two lowest curves based on the $1s\sigma_g$ and $2p\sigma_u$ MO are very similar to those for H_2^+. Again, the $1s\sigma_g$ is bonding and the lowest bound $L=0$ state will be shown to be of $^1S^e$ character. In H^-, however, the center of mass is practically at the proton, and the vibrational motion is that of a pair of electrons. Hence vibrational energies are of the order of electronic energies and this has the effect that only the rotationless ground vibrational state of H^- is bound. There is no further rovibrational bound spectrum. When one electron is removed from H^-, it "sees" a neutral ground-state H atom and this means that the $2p\sigma_u$ MO is fully antibonding as in H_2^+. The lowest triplet curve $^3S^e$ is built on this MO, as shown in Fig. 1.

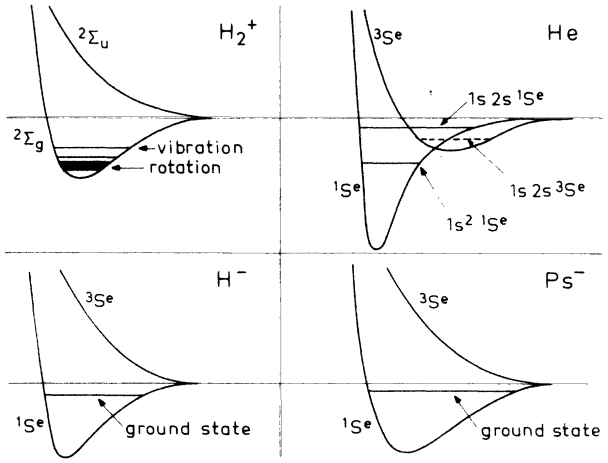

FIG. 1. Schematic representation of the lowest states built upon the $1s\sigma_g$ and the $2p\sigma_u$ MO for the three-body systems H_2^+, He, H^-, and Ps^-.

The system Ps^- is extremely similar to H^- in the MO model. The center of mass is shifted to the center of the "molecule," but the vibrational reduced mass and moment of inertia have the same order of magnitude as in H^-. Hence the structure of the lowest $^1S^e$ and $^3S^e$ curves based on $1s\sigma_g$ and $2p\sigma_u$ are qualitatively similar to H^-. The system Ps^- is simply a little larger, due to the smaller reduced mass of the "electronic" mode.

A dramatic change in the spectrum occurs when one considers the helium atom. This is due to the change in charge ratios arising from a nucleus with $Z=2$. An electron removed from the system ($R \to \infty$) "sees" the attractive Coulomb potential of ground-state He^+ which can support an infinity of bound states. Now both $1s\sigma_g$ and $2p\sigma_u$ are bonding orbitals and support potential wells. For $L=0$, the $1s\sigma_g$ gives rise to $^1S^e$ helium states and the $2p\sigma_u$ to $^3S^e$ states. Hence the $(1s^2)^1S^e$ ground state is the lowest vibrational state in the $1s\sigma_g$ potential well and the $(1s2s)\,^1S^e$ is the first excited vibrational state, and is bound, of course. The lowest triplet state $(1s2s)^3S^e$ is the ground vibrational state of the $2p\sigma_u$ potential well. The fact that this *ungerade* orbital supports the triplet state (and is antibonding for $Z=1$) explains qualitatively why the lowest triplet state of helium lies so far above the ground singlet state. The higher states with $L\neq 0$ are simply the singly excited states of helium converging to the $He^+(1s)$ threshold and are represented in the MO model by the manifold of rovibrational states built upon the $1s\sigma_g$ and $2p\sigma_u$ MO.

Some of the lower members of the singly excited series were discussed by Hunter and Pritchard,[20] and the states converging to the $N=2$ threshold were described in I. In the rest of this paper, the MO model will be discussed in more detail, with particular reference to the internal quantum numbers that it provides and to the scaling property of the MO adiabatic potential curves. In addition, the atomic transitions giving photon absorption and autoionization will be discussed in the language of molecular quantum mechanics. Then it appears that absorption to Rydberg series can be described in terms of vibrational progressions and Franck-Condon factors. The process of atomic autoionization is the direct analog of molecular dissociation. In this way, the description of atomic structure and transition processes finds a very close similarity to the conventional description of molecular structure and transition processes.[21] Atomic units will be used.

II. THE THREE-BODY COULOMB PROBLEM IN MOLECULAR COORDINATES

A. Coupled equations in an adiabatic basis

The three-body Coulomb problem will first be expressed in molecular coordinates for the case of arbitrary charges and masses and then specialized to the case in which two of the particles are electrons and the third has a positive charge. The molecular coordinates are such

that $\mathbf{R}$ is the vector separation of particles 1 and 2 of like charge ($Z_1Z_2>0$) and $\mathbf{r}$ is the separation of particle 3 of opposite charge ($Z_1Z_2Z_3<0$) from the center of mass of particles 1 and 2. The center-of-mass motion of the three-particle molecule is readily separated and the internal motion is specified by a wave function $\Phi(\mathbf{r},\mathbf{R})$ satisfying the Schrödinger equation

$$\left[-\frac{1}{2\mu_{12}}\nabla_{\mathbf{R}}^2-\frac{1}{2\mu_{12,3}}\nabla_{\mathbf{r}}^2+\frac{Z_1Z_2}{R}+\frac{Z_1Z_3}{r_1}+\frac{Z_2Z_3}{r_2}\right]\times\Phi(\mathbf{r},\mathbf{R})=E\Phi(\mathbf{r},\mathbf{R}) , \quad (2.1)$$

where

$$\mu_{12}=\frac{m_1m_2}{m_1+m_2}, \quad \mu_{12,3}=\frac{(m_1+m_2)m_3}{m_1+m_2+m_3}$$

are appropriate reduced masses and $\mathbf{r}_i=(\mathbf{r}\pm\mu_{12}\mathbf{R}/m_i)$ for $i=1,2$. In these Jacobi coordinates, the three-body Coulomb problem is identical to the fundamental problem of quantum chemistry, exemplified by the H_2^+ molecular ion. In that case, $Z_1=Z_2=+1$ and $Z_3=-1$. As such, the solution of the problem (2.1) has been discussed in great detail. The wave functions (2.1) can be characterized by eigenvalues of the energy E, total angular momentum $\mathbf{J}$ and its projection J_z along the space-fixed z axis. We will consider a situation in which total orbital momentum and spin can be uncoupled so that $\mathbf{L}$, L_z, $\mathbf{S}$, and S_z are also separately good quantum numbers. As in molecular calculations, it is convenient to consider the six-dimensional $\mathbf{r}$, $\mathbf{R}$ space in terms of three Euler angles ψ,Θ,ϕ (which rotate from a space-fixed to a body-fixed frame with the z axis along $\mathbf{R}$), the length R itself, and the coordinates r, Θ_r, ϕ_r of $\mathbf{r}$ in the body-fixed frame. Then it is clear that $\phi_r=\phi$ so that upon specification of the Euler angles, $\mathbf{r}$ is specified by *two* coordinates in the body-fixed $(\mathbf{R},\mathbf{r})$ plane. In these six coordinates, the total wave function for given energy can be further decomposed as

$$\Phi_{JM_J}(\mathbf{r},\mathbf{R})=\sum_{M,M_S}\Psi_{LM}(\mathbf{r},\mathbf{R})\chi_{SM_s}\langle LM\,SM_s\,|\,JM_J\rangle , \quad (2.2)$$

where χ_{SM_s} is a two-electron spin wave function. The spatial wave function Ψ_{LM} can be written as an infinite sum of product wave functions describing the rotation, vibration, and MO motions,

$$\Psi_{LM}(\mathbf{r},\mathbf{R})=\sum_K\sum_i D^L_{MK}(\psi,\Theta,0)R^{-1}f^L_{iK}(R)\phi_{iK}(\mathbf{r},R) . \quad (2.3)$$

The functions D^L_{MK} are rigid-top wave functions describing the rotation of the three-body system with total angular momentum $\mathbf{L}$. They are eigenfunctions of $\mathbf{L}^2$ with eigenvalue $L(L+1)$ and eigenfunctions of L_z with eigenvalues M and K in the space-fixed and body-fixed frames, respectively. The functions ϕ_{iK} are the MO wave functions describing the motion of $\mathbf{r}$ for fixed R. They are eigenfunctions of l_z, where

$$\boldsymbol{l}=-i\mathbf{r}\times\nabla_{\mathbf{r}} . \quad (2.4)$$

The total angular momentum is decomposed as

$$\mathbf{L}=\mathbf{L}_R+\boldsymbol{l} , \quad (2.5)$$

where $\mathbf{L}_R=-i\mathbf{R}\times\nabla_{\mathbf{R}}$. Since the z component of $\mathbf{L}_R$ is zero by definition of the body-fixed frame [$\mathbf{L}_R\cdot\hat{\mathbf{R}}\equiv0$], then l_z has the same eigenvalues K as L_z. Accordingly, the label i represents the quantum numbers associated with the other two degrees of freedom of $\mathbf{r}$. The functions $R^{-1}f^L_{iK}(R)$ describe the vibration of the coordinate R between the particles of like charge. It depends on the MO character specified by the labels i and K and upon the magnitude of the total angular momentum L.

The total Hamiltonian in (2.1) is written

$$H=-\nabla_R^2/(2\mu_{12})+h , \quad (2.6a)$$

where

$$h=-\nabla_r^2/(2\mu_{12,3})+Z_1Z_2/R+Z_1Z_3/r_1+Z_2Z_3/r_2 . \quad (2.6b)$$

The kinetic energy operator associated with $\mathbf{R}$ can be further separated into radial and angular parts,

$$-\nabla_R^2/(2\mu_{12})=P_R^2/(2\mu_{12})+\mathbf{L}_R^2/(2\mu_{12}R^2) . \quad (2.7)$$

The angular momentum $\mathbf{L}_R^2$ is written from (2.5) as

$$\begin{aligned}L_R^2&=\mathbf{L}^2+l^2-\mathbf{L}\cdot\boldsymbol{l}-\boldsymbol{l}\cdot\mathbf{L}\\&=\mathbf{L}^2+l^2-2L_z^2-L_+l_--l_+L_- .\end{aligned} \quad (2.8)$$

Since the spin is decoupled, the solution of the eigenvalue equation $(H-E)\Psi_{LM}=0$ reduces to the solution of the following set of coupled equations, after integration over the Euler angles and over $\mathbf{r}$:

$$\begin{aligned}&\{\partial^2/\partial R^2-2\mu_{12}[U^L_{iK}(R)-E]\}f^L_{iK}(R)\\&\quad=-\sum_{j\neq i}[\langle\phi_{iK}\,|\,\partial^2/\partial R^2+l^2/R^2\,|\,\phi_{jK}\rangle+\langle\phi_{iK}\,|\,(2/R)\partial/\partial R\,|\,\phi_{jK}\rangle\partial/\partial R]f^L_{jK}(R)\\&\qquad-\Lambda_+\langle\phi_{iK}\,|\,l_-\,|\,\phi_{jK+1}\rangle f^L_{jK+1}(R)-\Lambda_-\langle\phi_{iK}\,|\,l_+\,|\,\phi_{jK-1}\rangle f^L_{jK-1}(R) ,\end{aligned} \quad (2.9)$$

where

$$\Lambda_\pm=[(L\mp K)(L\pm K+1)]^{1/2} .$$

The diagonal energy U^L_{iK} appearing on the left-hand side (lhs) of (2.9) is defined by the matrix element,

$$\langle\phi_{iK}\,|\,h+(2\mu_{12})^{-1}\{-\partial^2/\partial R^2+[L(L+1)-2K^2+l^2]/R^2\}\,|\,\phi_{iK}\rangle=U^L_{iK}(R) . \quad (2.10)$$

It should be noted that ϕ_{iK} depends on L, although it is not an eigenfunction of $\mathbf{L}^2$. The nondiagonal terms appearing on the right-hand side (rhs) of (2.9) are usually called radial coupling terms ($\Delta K=0$) or rotational or Coriolis couping terms ($\Delta K=\pm 1$).

In the molecular case (particles 1 and 2 being nuclei, particle 3 being an electron) the complexity of (2.9) and (2.10) is usually drastically reduced by making the Born-Oppenheimer (BO) approximation. This involves the recognition that μ_{12} is of the order of a nuclear mass and $\mu_{12,3}$ is of the order of electron mass. This justifies a systematic neglect of terms involving μ_{12}^{-1}. Then Eq. (2.10) reduces to the BO energy,

$$\langle \phi_{iK} \mid h \mid \phi_{iK} \rangle = \epsilon(R) \ . \tag{2.11a}$$

By the same argument, all nondiagonal terms in (2.9) may be neglected, and the simple radial equation

$$\{\partial^2/\partial R^2 - 2\mu_{12}[\epsilon(R)-E]\} f_{iK}(R) = 0 \tag{2.11b}$$

is solved for the vibrational wave function and associated vibrational energies. There remains the rotational energy represented by the centrifugal term in (2.10). This energy contribution is added by calculating its expectation value in the wave functions obtained from (2.11). Thus the BO approximation makes a clear separation between MO (electronic), vibrational, and rotational motion of the molecular ion.

We now consider to what extent Eqs. (2.9) and (2.10) can be approximated in our system of interest, namely, two electrons and one nucleus. In this case, $\mathbf{R}$ is the interelectronic axis and $\mathbf{r}$ describes the motion of the electronic center of mass with respect to the nucleus. The most obvious change with respect to H_2^+ is in the reduced mass μ_{12}, which is now equal to $\frac{1}{2}$ (in atomic units), although $\mu_{12,3}$ only changes from 1 to 2 in the cases of He and H^- and from 1 to $\frac{2}{3}$ in the case of Ps^-. Clearly, the BO approximation cannot now be made and Eq. (2.10) must be solved. Solutions of this equation which, in contrast to BO solutions, have the exact asymptotic SA behavior, have been called adiabatic MO.[22] Having obtained these adiabatic MO solutions, there is no apparent reason for dropping the off-diagonal nonadiabatic terms in (2.9), as is justified in the molecular case by the inertia of the internuclear axis. Some justification can be obtained, however, by observing that off-diagonal coupling elements are proportional to the energy difference between the relevant levels (this can be seen explicitly by applying the Hellman-Feynman theorem to matrix elements $\langle \phi_{iK} \mid \partial/\partial R \mid \phi_{jK} \rangle$, for example). Hence, so long as distinct adiabatic MO's are energetically well separated from other MO's, the adiabatic single-channel approximation should be good. It will always break down, in principle, at crossings of adiabatic MO's. In specific cases, however, symmetry or dynamical considerations indicate that the interaction is zero or highly localized. It is on this basis that we will discuss the properties of two-electron atomic states in terms of the symmetries and energies of molecular states based on the single-channel adiabatic solutions of Eqs. (2.9) and (2.10). Moreover, that the validity of the Born-Oppenheimer approximation in general has very little to do with the appearance of small mass ratios has been suggested by Essén.[23] This work shows that it is the form of the interaction between the particles, and not mass ratios, that is responsible for the approximate separation of an adiabatic coordinate. In particular, it is the repulsive form of the nuclear interaction that is ultimately responsible for molecular structure. The interaction potentials in two-electron atoms are identical to those in H_2^+ and Essén's analysis would imply that it is the rigidity of the interelectronic axis arising from the interelectronic repulsion that accounts for the approximate separability in the atomic case. This will be particularly true in the case of doubly excited atomic states, where a large interelectronic separation implies that centrifugal and Coriolis couplings, proportional to R^{-2}, are relatively unimportant.

B. MO symmetries and two-electron atomic wave functions

The overall symmetry of the atomic states is the first consideration. At the level of energy resolution of interest here, the nuclear spin can be neglected. Thus the total spin S of the atom is that of the two electrons alone. Furthermore, the total parity of the atom is a good quantum number. Hence the atomic spatial wave functions must be eigenfunctions of the electron exchange operator P_{12} and the parity operator P. As explained in the Introduction, we also wish to emphasize the product of these two operations, PP_{12}, which corresponds to the g-u symmetry of the MO. In the $\mathbf{r},\mathbf{R}$ coordinates, these three operations are defined by

$$P:\mathbf{R}\rightarrow -\mathbf{R},\mathbf{r}\rightarrow -\mathbf{r} \ , \tag{2.12a}$$

$$P_{12}:\mathbf{R}\rightarrow -\mathbf{R},\ \mathbf{r}\rightarrow \mathbf{r} \ , \tag{2.12b}$$

$$PP_{12}:\mathbf{R}\rightarrow \mathbf{R},\ \mathbf{r}\rightarrow -\mathbf{r} \ . \tag{2.12c}$$

It is clear that the total Hamiltonian (2.6) is invariant under these operations, only two of which are independent of course. Total spatial wave functions which are also eigenfunctions of the above operators (2.12) are constructed as follows:

$$\Psi_{LM}(\mathbf{r},\mathbf{R}) = \sum_K \sum_i [D^L_{MK} + (-1)^{S+t+L+K} D^L_{M-K}] \times R^{-1} f^L_{iK}(R) \phi_{iK}(\mathbf{r},R) \ . \tag{2.13}$$

These functions are symmetric ($S=0$) or antisymmetric ($S=1$) according to the eigenvalues $(-1)^S$ of P_{12}. These functions have *gerade* ($t=0$) or *ungerade* ($t=1$) symmetry according to the eigenvalues $(-1)^t$ of PP_{12}. Since t is a good quantum number for the atom as a whole, MO's of different g,u symmetry do not couple. The parity operator P has eigenvalues $\pi=\pm 1$, given by $\pi=(-1)^{S+t}$, and is here viewed as being derived from the other two symmetry operations (2.12b) and (2.12c). This is analogous to the specification of parity as $\pi=(-1)^L$, where $L=\sum l_i$ in the independent-electron picture.

The quantum number t is the only MO "internal" quantum number which remains a good quantum number

of the two-electron atom. However, the MO decomposition gives further approximate quantum numbers. Of these, the orbital projection quantum number K assumes a place of special importance, as it appears not only in the rotational-wave function but also characterizes the adiabatic MO. An essential feature of the molecular model is the goodness of the quantum number K, i.e., the absence of extensive rotational coupling. In addition to K, however, the adiabatic MO model furnishes other quantum numbers whose significance for the classification of two-electron states is indicated below.

As has been shown,[14,20,22,24] the adiabatic MO in Eq. (2.10) can be obtained by a variational procedure from trial functions having the analytic form of eigenfunctions of the BO Hamiltonian h, given by (2.6b), for fixed values of R. This procedure is discussed in more detail in Sec. III. The adiabatic MO then possess the same symmetries as these BO solutions. In addition to the g,u symmetry corresponding to their behavior under reversal of the vector $\mathbf{r}$ and to the K quantum number which is the eigenvalue of l_z and L_z, there are two further MO quantum numbers. These arise from the separability of the Hamiltonian h in the confocal elliptic coordinates

$$\lambda=(r_1+r_2)/R \ , \tag{2.14}$$

$$\mu=(r_1-r_2)/R \ . \tag{2.15}$$

This separation of the BO two-center problem and the eigensolutions of the separated equations in λ and in μ have been discussed very extensively.[25–27] The λ or outer solution has elliptical nodal surfaces with the two electrons as foci. The solution in μ has corresponding hyperbolic nodal surfaces. An important point is that the number n_λ, n_μ of these nodal surfaces is conserved for all R and, as indicated in Fig. 2, allows one to connect SA and UA ($R=0$) atomic limits (the correlation diagram of molecular physics). The number of nodes n_ϕ in ϕ is similarly independent of R, so that the MO quantum number K is just the magnetic quantum number of both SA and UA limits. In the UA limit, the coordinates become the spherical polar coordinates. Then $n_\lambda=n_r=n-l-1$, the number of radial spherical nodes, and $n_\mu=l-|m|$, the number of polar nodes in Θ. In the SA limit, the coordinates become the Stark-state parabolic ones. The two parabolic quantum numbers are $n_1=n_\lambda$ and $n_2=n_\mu/2$ if n_μ is even and $(n_\mu-1)/2$ if n_μ is odd. The connection[27] between SA, Stark, MO, and UA quantum numbers is given in Fig. 2 for the $N=1$ and 2 SA states.

The g,u symmetry can also be given a simple interpretation in terms of the UA behavior of MO's. From the correlation diagram, it is readily seen that $(-1)^t=(-1)^l$, the united atom parity. Hence the specification of a MO by the UA quantum numbers n,l,K is sufficient to define n_λ, n_μ, K, and t uniquely. Despite this redundancy, the index g ($t=0$) or u ($t=1$) is usually added to a MO designation to indicate this symmetry explicitly.

There remains an additional MO quantum number which is present only in the case of pure Coulomb forces.

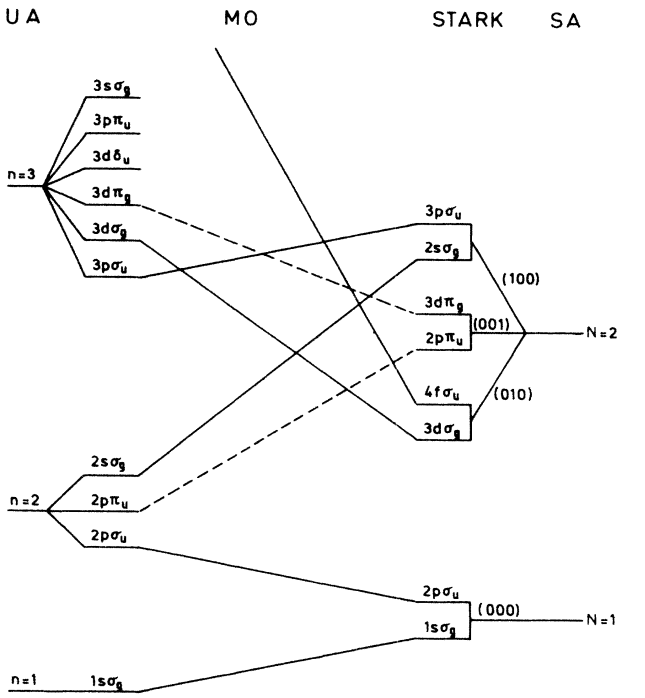

FIG. 2. Correlation diagram of the MO emanating from the $N=1$ and 2 hydrogenic levels for the three-body systems H_2^+, He, H^-, and Ps^-.

This is related to the Runge-Lenz vector and is discussed in more detail below. Unlike the other MO quantum numbers, it is a function of the interelectronic distance R and is not, in general, an integer. Its presence signifies the separability of the adiabatic MO equation in λ,μ coordinates. We will denote this quantum number as the expectation value $\langle\Omega(R)\rangle$ of an operator $\Omega(R)$ (defined below) for fixed R.

Finally, from the solution of the coupled equations (2.9) will emerge a sequence of energy eigenvalues. In the uncoupled, single MO approximation, these will be the sequence of vibrational levels with quantum number ν appearing as the vibrational eigenvalues in a given MO potential of fixed L. Hence the sequence of quantum numbers n_λ, n_μ, K, t, $\langle\Omega(R)\rangle$, and ν specifies a set of approximate symmetries of the internal motion for a given state of $LS\pi$ symmetry. The symmetries are broken by radial and rotational coupling. More correctly, all are broken except the symmetry corresponding to t, since $(-1)^t=\pi(-1)^S$. The origin of the preservation of the overall g,u symmetry is to be traced to the fact that the $\mathbf{r},\mathbf{R}$ are Jacobi coordinates and hence the usual two-electron Hamiltonian in $\mathbf{r}_1,\mathbf{r}_2$ coordinates,

$$H=-\tfrac{1}{2}\nabla_{r_1}^2-\tfrac{1}{2}\nabla_{r_2}^2+V_{13}(r_1)+V_{23}(r_2)+V_{12}(R) \ , \tag{2.16}$$

is obtained by direct transformation of (2.6) and neglect in He and H^- of terms of the order of inverse nuclear mass [cf. Eq. (3.2)]. Naturally, (2.16) is also invariant under the operation PP_{12} which takes $\mathbf{r}$ into $-\mathbf{r}$, although this is not usually emphasized.

C. MO interpretation of previous classification schemes

The set of approximate internal MO symmetries in our molecular model plays a role similar to the more usual approximate symmetries represented by one-electron quantum numbers (n_1,l_1,m_1) and (n_2,l_2,m_2) of the atomic independent-electron description. As outlined in the Introduction, apart from the use of configuration interaction based on an independent-electron model,[2] two methods have been used to discuss doubly excited states of two-electron atoms. The first is the adiabatic separation in hyperspherical coordinates (reviewed in Ref. 1), which has shown good numerical accuracy but isolates no internal symmetries. The second method[10,28,29] concentrates on the explicit introduction of approximate symmetries based upon particular dynamical models. This method has been successful in identifying certain symmetries by which groups of two-electron states may be classified but has no power to make *ab initio* calculations. The molecular model provides not only a complete set of symmetry properties and a simple explanation of previously identified symmetries but also a calculational prescription.

Guided by the group-theoretical analysis of Herrick and co-workers and by the molecular approach,[13,14] Watanabe and Lin[18] extracted approximate internal symmetries for two-electron wave functions. They identified not only the two quantum numbers T and K_H that were proposed by Herrick and co-workers, but an additional quantum number A, originally proposed by Lin[5(d)] empirically from a study of calculated hyperspherical adiabatic wave functions. We can give a direct and much simpler MO explanation of the existence of the quantum numbers T, A, and K_H.

The quantum number T is the body-frame molecular angular momentum projection quantum number. In line with molecular notation, we call this projection K, and it is defined by the molecular rotational-wave function D^L_{MK}. In the MO model, however, the projection of total angular momentum $\mathbf{L}$ along the interelectronic axis is identical to the projection of the electronic center-of-mass angular momentum l along this axis. That is, K is also an internal MO quantum number denoting the σ, π, etc., character of the MO and is equal to the UA and SA magnetic quantum numbers. Hence, in the MO model, the quantum number K can be associated directly with the adiabatic potential curves.

The quantum numbers A and K_H can be expressed in terms of the two MO quantum numbers n_λ,n_μ, which specify the number of elliptic and hyperbolic nodal surfaces, respectively. As mentioned before, these surfaces are conserved for all R and n_λ,n_μ can be connected directly to the SA and UA quantum numbers.

Lin[5(d)] identified empirically a property of hyperspherical wave functions to which he gave the label A with values $+$, $-$, or 0. Later, Watanabe and Lin[18] identified the first two cases as the sign of $A=\pi(-1)^{S+T}$, where in their notation T is the angular momentum projection quantum number. Hence, in our notation, $A=\pi(-1)^{S+K}$. However, we have seen that $\pi(-1)^S=(-1)^t$ denotes the g or u character of the two-electron state. Furthermore, $(-1)^t$ is equal to $(-1)^l$, where l is the UA orbital angular momentum, i.e., $(-1)^l$ is the UA parity. Therefore we can write

$$A=(-1)^{l+K}=(-1)^{l-K}=(-1)^{n_\mu} . \tag{2.17}$$

Accordingly, we have related Lin's A quantum number to the number of hyperbolic MO surfaces for the cases $A=+$ or $-$. Note that for n_μ odd, there is a node where $\mu=0$, i.e., $r_1=r_2$. The case A equal to zero does not arise in the MO description.

The quantum number K_H was first suggested on the basis of the algebraic structure of the product group $[O(4)]_1\times[O(4)]_2$ for two electrons in a Coulomb field. It was further interpreted in terms of the triatomic rovibrational model by Watanabe and Lin,[18] and recently discussed by Mølmer and Taulbjerg.[29] If N is the SA principal quantum number, it can be shown that K_H assumes the values

$$K_H=(N-T-1),(N-T-3),\ldots,-(N-T-1) . \tag{2.18}$$

Again in our notation $T\equiv K$ the angular momentum projection quantum number of the MO. However, this quantum number is preserved for all R and hence $T\equiv K=|m|$, where m is the SA magnetic quantum number. Hence

$$K_H=(N-|m|-1),(N-|m|-3),\ldots,-(N-|m|-1) . \tag{2.19}$$

However, $(N-|m|-1)=n_1+n_2$, the sum of the two SA parabolic quantum numbers. Further, the sequence (2.19) is equivalent to the sequence generated by

$$K_H=(N-|m|-1)-2n_1=n_2-n_1 \tag{2.20}$$

for the allowed values of n_1 and n_2. This extremely simple interpretation of K_H appears to have gone unnoticed. The presence of K_H also depends upon the presence of a pure Coulomb interaction in the separated atom, i.e., the limit $R\rightarrow\infty$ when one electron has been removed from the two-electron atom. This is seen by noting that for a parabolic one-electron SA state $|Nn_1n_2m\rangle$, we have

$$\begin{aligned} a_z|Nn_1n_2m\rangle&=[(n_2-n_1)/N]|Nn_1n_2m\rangle \\ &=(K_H/N)|Nn_1n_2m\rangle , \end{aligned} \tag{2.21}$$

so that K_H is simply proportional to the z component of the SA Runge-Lenz vector $\mathbf{a}$ [defined in (2.26)].

Since there exists a one-to-one correspondence between the SA parabolic quantum numbers and the MO quantum numbers, then K_H can be expressed also in terms of n_λ, n_μ, and K as the sequences generated by

$$K_H=(N-K-1)-2n_\lambda , \tag{2.22}$$

since $n_1=n_\lambda$ or, in addition, since $n_2=n_\mu/2$ for n_μ even, and $n_2=(n_\mu-1)/2$ for n_μ odd,

$$K_H = n_2 - n_1 = \begin{cases} (n_\mu/2) - n_\lambda, & n_\mu \text{ even} \\ [(n_\mu - 1)/2] - n_\lambda, & n_\mu \text{ odd} \end{cases} . \quad (2.23)$$

Using the connection $n_\lambda = n - l - 1$ and $n_\mu = l - K$ to UA quantum numbers, one can also express K_H in terms of these quantum numbers.

To summarize, we have explained Lin's K_H, A, and T quantum numbers, derived either empirically or from group theory, in terms of the good MO quantum numbers n_λ, n_μ, and K. Historically, the quantum number K_H was derived from independent-electron, or separated-atom, considerations but used to label hyperspherical curves for all $\mathcal{R}$. The conservation of nodal surfaces for all R in the MO model and the consequent connection of MO and parabolic [O(4)] quantum numbers leading to (2.20) and (2.23) justify the use of K_H for labeling two-electron states. However, the simplicity of the MO picture and the connection to SA and UA limits suggests the use of n_λ, n_μ, and K as a more natural classification scheme of two-electron states.

There remains a further constant of the motion in the MO model. This arises from the separability of the BO Hamiltonian in elliptic coordinates λ, μ and, indeed, is related to the separation constant itself, for fixed R. This additional quantity has been discussed by many authors (see, for example, Coulson and Joseph[30]). For our case of two electrons and one nucleus of charge Z, it is conveniently expressed as the operator

$$\Omega(R) = \tfrac{1}{2}(\mathbf{l}_1 \cdot \mathbf{l}_2 + \mathbf{l}_2 \cdot \mathbf{l}_1) + Z\mathbf{R} \cdot (\hat{\mathbf{r}}_1 - \hat{\mathbf{r}}_2) , \quad (2.24)$$

where $\mathbf{l}_1 = -i\mathbf{r}_1 \times \nabla_{\mathbf{r}_1}$ and $\mathbf{l}_2 = -i\mathbf{r}_2 \times \nabla_{\mathbf{r}_2}$. This operator commutes with h, the BO Hamiltonian. The existence of this dynamical constant of the motion for each fixed R leads to the crossing of certain MO's despite their similar geometrical symmetry, e.g., the $2s\sigma_g$ and $3d\sigma_g$ MO. The separation constant of the BO equation at each value of R is given by the MO expectation value of the operator $-(\Omega + R^2 h/4)$.

The operator (2.24) may be written in several forms. For example,

$$\Omega = (\mathbf{l}_1 + \mathbf{l}_2)^2/4 - (\mathbf{l}_1 - \mathbf{l}_2)^2/4 + Z(r_1 + r_2)(1 - \cos\Theta_{12}) , \quad (2.25)$$

which emphasizes its dependence on the individual angular momenta and the angular correlation via the dependence on $\Theta_{12} = \cos^{-1}(\hat{\mathbf{r}}_1 \cdot \hat{\mathbf{r}}_2)$. A connection with the one-electron SA Runge-Lenz vector

$$\mathbf{a}_i = i(\mathbf{l}_i \times \nabla_{\mathbf{r}_i} - \nabla_{\mathbf{r}_i} \times \mathbf{l}_i) - Z\hat{\mathbf{r}}_i \quad (2.26)$$

may also be made by transforming (2.24) to the form

$$\Omega = (\mathbf{l}_1 + \mathbf{l}_2)^2/4 - 3(\mathbf{l}_1 - \mathbf{l}_2)^2/4 + \mathbf{R} \cdot (\mathbf{a}_2 - \mathbf{a}_1)/2 . \quad (2.27)$$

The forms (2.24) and (2.27) show clearly that in the UA limit $R \to 0$, $\Omega \to l^2$, where $\mathbf{l}_1 = \mathbf{l}_2 = \mathbf{l}$ is the UA orbital angular momentum operator. In the SA limit $R \to \infty$, one can also show[26] that Ω has asymptotic behavior such that

$$\frac{C}{R} - 1 \to \frac{n_2 - n_1}{N} , \quad (2.28)$$

where C is the expectation value of the operator $-(\Omega + R^2 h/4)$, i.e., C is the asymptotic value of the BO separation constant. From Eq. (2.21), one recognizes that the rhs of (2.28) is the eigenvalue of a_z for the SA. Hence the asymptotic form of $\langle \Omega(R) \rangle$, the two-center dynamic constant of the motion, also explains the existence of Herrick's quantum number K_H.

III. CONSTRUCTION OF ATOMIC STATES AND ADIABATIC POTENTIALS

A. Atomic states in a MO description

The MO's are characterized by the quantum numbers K, t, n_λ, and n_μ. The validity of these quantum numbers for all R allows the correlation diagram of Fig. 2 to be drawn (a more extensive correlation diagram is given by Barat and Lichten[31]). In Sec. III B we will show how single-channel adiabatic molecular energy curves can be constructed from calculated MO energies. However, the atomic states that are supported by each MO can be simply derived from the MO quantum numbers and a consideration of the form (2.13) of the total spatial wave function for each component labeled by iK, where i denotes the set of quantum numbers n_λ, n_μ, and t.

Quite generally, the MO's appear in pairs of g,u symmetry ($t=0$ or 1, respectively) separating to specific Stark states. The lowest pair is the $1s\sigma_g$, $2p\sigma_u$ pair separating to the $1s$ level and correlating to the UA $1s$ and $2p_0$ levels, respectively. The MO $1s\sigma_g$ has quantum numbers $K=0$, $t=0$, $n_\lambda=0$, and $n_\mu=0$ and therefore no nodal surfaces. Since K and t are zero, one sees from (2.13) that only states where $(L+S)$ is even are allowed. The parity is given by $\pi = (-1)^{S+t} = (-1)^S$. Hence the sequence of states ${}^1S^e$, ${}^3P^o$, ${}^1D^e$, ${}^3F^o$ etc., is based upon the $1s\sigma_g$ MO. The $2p\sigma_u$ MO has $K=0$, $t=1$, $n_\lambda=0$, and $n_\mu=1$. Hence, from (2.13), only states where $(L+S)$ is odd and $\pi = (-1)^{S+1}$ are allowed, i.e., the sequence ${}^3S^e$, ${}^1P^o$, ${}^3D^e$, ${}^1F^o$, etc. The form of (2.13) indicates that for given L and S, only the MO quantum numbers K and t are relevant in deciding the allowed atomic states. Hence all MO's of σ_g symmetry will give rise to the sequence ${}^1S^e$, ${}^3P^o$, ${}^1D^e$, ${}^3F^o$, etc., and all MO's of σ_u symmetry to the sequence ${}^3S^e$, ${}^1P^o$, ${}^3D^e$, ${}^1F^o$, etc. This analysis (which was given in I) explains our association of the lowest ${}^1S^e$ and ${}^3S^e$ levels of He, H^-, and Ps^- with the $1s\sigma_g$ and $2p\sigma_u$ MO's, respectively, as shown in Fig. 1.

As shown in Fig. 2, the pairs $2s\sigma_g, 3p\sigma_u$ and $3d\sigma_g, 4f\sigma_u$ correlate to the $n=2$ SA levels, and these will give rise to the sequences of states discussed above. Pairs of states with $K \neq 0$ give rise to two sequences of states, according to whether $t=0$ or 1. They have parity $\pi = (-1)^{S+t}$ and are subject to the restriction $L \geq |K|$. Hence all states of π_g symmetry give rise to sequences ${}^1P^e$, ${}^3P^o$, ${}^1D^e$, ${}^3D^o$, etc., and all states of π_u symmetry to sequences ${}^3P^e$, ${}^1P^o$, ${}^3D^e$, ${}^1D^o$, etc. The sequences of states built upon g,u pairs of higher K value are the same, but with the components with $L < K$ missing. We note that the above sequences are the same as those derived by Herrick *et al.*[9] on the basis of group theory.

In Sec. III B the calculation of single-channel adiabatic

curves for atomic states based upon MO separating to the SA $N=2$ manifold is described and the results are used to interpret certain features of the corresponding hyperspherical adiabatic potential curves.

B. Construction of the adiabatic potentials

The single-channel "molecular" potential energy curves as a function of interelectronic distance R are obtained as the functions $U_{iK}^{L}(R)$ from Eq. (2.10). As is well known, the BO solutions of (2.11a) do not have the correct form as $R\rightarrow\infty$, the SA limit. This is true even in the molecular case and arises from the fact that BO solutions tend to separated-atom functions with the wrong reduced mass for the electron-nucleus motion. This deficiency of the BO solutions has been discussed many times in the molecular case[14(a),20,22,24,32–34] where it gives a small dependence of energies upon isotopic masses. In the atomic case (I and Feagin and Briggs[14]), it leads to large errors, since the MO reduced mass μ_{12} is equal to $\frac{1}{2}$, whereas the separated-atom reduced mass is close to unity. The error made in the BO approximation is to ignore the diagonal matrix elements of the kinetic energy operator $(2\mu_{12})^{-1}\nabla_R^2$. This inclusion is necessary since only the full kinetic energy operator

$$-\frac{1}{2\mu_{12,3}}\nabla_r^2-\frac{1}{2\mu_{12}}\nabla_R^2 \tag{3.1}$$

transforms correctly to the full kinetic energy in the Jacobi coordinates of the separated-atom configuration, i.e.,

$$-\frac{1}{2\mu_{13,2}}\nabla_{r_2}^2-\frac{1}{2\mu_{13}}\nabla_{r_1}^2\ , \tag{3.2}$$

where $\mathbf{r}_1$ is the separation of electron 1 and the nucleus, and $\mathbf{r}_2$ is the separation of electron 2 from the center of mass of electron 1 and the nucleus. Equation (2.10) contains the full kinetic energy operator (3.1) and therefore, in the large-R limit, does contain the correct asymptotic kinetic energy $-(2\mu_{13})^{-1}\nabla_{r_1}^2$ of the separated atom.

Since our emphasis here is on the symmetries provided by the MO description of the internal $\mathbf{r}$ motion, we will solve (2.10) approximately, by using a trial function of the BO analytic form provided by eigensolutions of the BO Hamiltonian h. Specifically, following Hunter and Pritchard,[20] we will assume trial functions of the form of H_2^+ MO solutions (with $Z=1$ and $\mu_{12,3}=1$) and introduce a scaling of the lengths $\mathbf{r}$ and $\mathbf{R}$. In this way, we will show that we can construct adiabatic MO potential curves for the systems He, H^-, and Ps^-, simply by scaling the quantities presented[27] in the literature for the H_2^+ molecular ion. This procedure has the advantage that we do not have to derive the rather complicated form of the BO wave function for each system separately. Furthermore, it shows that the qualitatively similar adiabatic potential curves for H_2^+, He, H^-, and Ps^- are related by a relatively simple scaling relation.

For brevity, in the following, we shall write μ for $\mu_{12,3}$. Furthermore, we will drop the MO subscripts iK on the wave functions $\phi(\mathbf{r},R)$. Then (2.10) can be expressed as

$$\langle\phi\,|\,h+(2\mu_{12})^{-1}C_{\rm op}\,|\,\phi\rangle+1/R=U(R)\ , \tag{3.3}$$

where h is the BO Hamiltonian, written without the electron-electron repulsion

$$h=-\nabla_r^2/(2\mu)-Z/r_1-Z/r_2 \tag{3.4}$$

and $C_{\rm op}$ is the non-BO operator

$$C_{\rm op}=-\partial^2/\partial R^2+[L(L+1)-K^2+l_x^2+l_y^2]/R^2\ . \tag{3.5}$$

It is important, for the following, to note that (3.4) with $\mu=1$, $Z=1$ is just the BO Hamiltonian of H_2^+, for which the eigenvalues and eigenfunctions, i.e., the solutions of

$$h\psi(\mathbf{r},R)=\epsilon(R)\psi(\mathbf{r},R)\ , \tag{3.6}$$

are known. We will evaluate (3.3) by introducing an R-dependent parameter ζ into the H_2^+ BO solutions of (3.6), by which lengths are scaled as

$$S\equiv\mu Z\zeta R,\quad \mathbf{x}=\mu Z\zeta\mathbf{r} \tag{3.7}$$

and the BO wave functions as

$$\phi(\mathbf{r},R)=(\mu Z\zeta)^{3/2}\psi(\mathbf{x},S)\ . \tag{3.8}$$

Then with (3.4) the BO energy $\epsilon(R)$ scales as

$$\begin{aligned}\epsilon(R)&=\int d\mathbf{r}\,\phi(\mathbf{r},R)h\phi(\mathbf{r},R)\\&=\mu Z^2\int d\mathbf{x}\,\psi(\mathbf{x},S)[\zeta^2(-\nabla_x^2/2)\\&\qquad-\zeta(1/x_1+1/x_2)]\psi(\mathbf{x},S)\\&=\mu Z^2[\zeta^2T(S)+\zeta V(S)]\ ,\end{aligned} \tag{3.9}$$

where T and V are the $\mu=Z=\zeta=1$ expectation values of the BO kinetic and potential energies of the H_2^+ problem with $\epsilon(R)=T(R)+V(R)$. Thus the scaling requires the separate evaluation of the BO kinetic and potential energies.[20] Since these quantities are not tabulated separately for all MO's of interest, they were obtained from tabulated values[27] of $\epsilon(S)$ by use of the virial theorem,[32,35]

$$\begin{aligned}T(S)&=-\epsilon(S)-S\epsilon'(S)\ ,\\V(S)&=2\epsilon(S)+S\epsilon'(S)\ ,\end{aligned} \tag{3.10}$$

where $\epsilon'(S)$ is the derivative of $\epsilon(S)$ with respect to S.

Scaling the expectation value of $C_{\rm op}$ with respect to BO wave functions gives

$$\begin{aligned}C(R)&\equiv\langle\phi\,|\,C_{\rm op}(R)\,|\,\phi\rangle\\&=(\mu Z\zeta)^2\,\delta(S)\ ,\end{aligned} \tag{3.11}$$

where

$$\delta(S)\equiv\int\psi(\mathbf{x},S)C_{\rm op}(S)\psi(\mathbf{x},S)d\mathbf{x}\ . \tag{3.12}$$

With the results (3.9)–(3.11), the adiabatic potential for the BO problem with reduced mass μ and potential strength Z may be obtained from the H_2^+ expectation values $\epsilon(S)$, $\delta(S)$ as

$$\begin{aligned}U(R)=\mu Z^2\zeta[&(2-\zeta)\epsilon(S)+(1-\zeta)S\epsilon'(S)\\&+\mu\zeta\,\delta(S)/2\mu_{12}]+1/R\ .\end{aligned} \tag{3.13}$$

The parameter $\zeta(R)$ remains to be determined. This

can be done by a variational procedure at each R as described in detail by Rost and Briggs.[24] However, since our aim here is a qualitative comparison with hyperspherical adiabatic curves, we find it sufficient to evaluate ζ for $R\to\infty$ and use this value to scale H_2^+ curves for all R. This ensures the correct SA limit of the MO curves and is partially justified by the dominance of electronic repulsion at small R. For the $1s\sigma_g$ and $2p\sigma_u$ MO, a more accurate evaluation was performed[14(a)] and the differences from $U(R)$ obtained with $\zeta(R\to\infty)$ were not significant enough to alter any of the qualitative results described in Sec. III C.

We demonstrate explicitly how (2.10), evaluated with scaled H_2^+ BO wave functions, provides the correct $R\to\infty$ dissociation energies for two-electron atoms. In the SA limit, one finds[27] that

$$\lim_{S\to\infty}[S\epsilon'(S)]\to 0$$

and therefore, with $2\mu_{12}=1$, that

$$U(\infty)=-\mu Z^2[2(2\zeta-\zeta^2)-\mu\zeta^2]/(4N^2)\ , \tag{3.14}$$

since $\epsilon(\infty)=-1/(2N^2)$ and $\delta(\infty)=1/(4N^2)$. Then, minimizing $U(\infty)$ with respect to ζ, by requiring that $\partial U(\infty)/\partial\zeta=0$, yields

$$\zeta=2/(2+\mu)\ , \tag{3.15}$$

independent of N and Z. Substitution of (3.15) in (3.14) gives

$$U(\infty)=-[2\mu/(2+\mu)]Z^2/(2N^2)\ . \tag{3.16}$$

In the case of two electrons, where $R\to\infty$ implies that one of the electrons, say electron 1, remains bound to the nucleus (particle 3), the SA reduced mass is μ_{13}. However, one has

$$\mu\equiv\mu_{12,3}=2\mu_{13}/(2-\mu_{13})$$

or

$$\mu_{13}=2\mu/(2+\mu)\ . \tag{3.17}$$

Hence

$$U(\infty)=-\mu_{13}Z^2/(2N^2)\ , \tag{3.18}$$

which is the *exact* binding energy of a SA state with principal quantum number N. With (3.13), (3.15), and $\zeta=\zeta(\infty)=\mu_{13}/\mu$, we have an approximate expression for $U(R)$ in terms of the H_2^+ quantities $\epsilon(S)$ and $\delta(S)$.

$$U(R)=[2\mu Z/(2+\mu)]^2\times[(1+1/\mu)\epsilon(S)+S\epsilon'(S)/2+\delta(S)/2\mu_{12}]+1/R\ , \tag{3.19}$$

where

$$S=[2\mu/(2+\mu)]ZR=\mu_{13}ZR\ . \tag{3.20}$$

This result illustrates why the adiabatic potential curves for all the systems H_2^+, He, H^-, and Ps^- are qualitatively similar. In all cases, the values of μ and Z are of order unity. The major difference, as exemplified by Fig. 1, comes from helium's having $Z=2$ and hence a residual Coulomb potential in the SA limit. In Sec. III C the potential curves $U(R)$ of (3.19) are presented for the $N=2$ manifold of the systems He ($Z=2$, $\mu\approx 2$, $\mu_{13}\approx 1$), H^{-1} ($Z=1$, $\mu\approx 2$, $\mu_{13}\approx 1$), and Ps^- ($Z=1$, $\mu=\frac{2}{3}$, $\mu_{13}=\frac{1}{2}$), where the approximations are to within the inverse nuclear mass.

Finally, we remark that the scaled coordinates x and S of (3.7) ensure that the MO wave functions for large R decay as

$$\phi(\mathbf{r},R)\sim\exp(-x_1/N)\pm\exp(-x_2/N)=\exp(-\mu_{13}Zr_1/N)\pm\exp(-\mu_{13}Zr_2/N)\ , \tag{3.21}$$

corresponding to the proper linear combination of (hydrogenic) atomic orbitals (LCAO) with the *exact* SA reduced mass.

C. Molecular curves

In this section the scaled potential curves for H^-, Ps^-, and He are presented and used to interpret certain unexplained features of the corresponding curves calculated in terms of the hyperspherical radius. A preliminary account of these results was given in I. The H^- potential curves of ^1S, ^3S, ^1P, and ^3P symmetry converging to the $N=2$ level of hydrogen are shown in Fig. 3 in comparison to the hyperspherical results of Lin.[5(b)] The similarity of the curves, in the MO case as a function of interelectronic distance R, in Lin's case as a function of the hyperspherical radius $\mathcal{R}=(r_1^2+r_2^2)^{1/2}$, is striking. Among the most-discussed curves are those of $^1P^o$ symmetry, labeled $+$, $-$, and pd by Lin according to the earlier classification of Cooper *et al.*[3] In the MO classification, one sees that they are based, respectively, upon the $2p\pi_u$ MO (with quantum numbers $n_\lambda=0$, $n_\mu=0$, $K=1$), the $4f\sigma_u$ MO ($n_\lambda=0$, $n_\mu=3$, $K=0$), and the $3p\sigma_u$ MO ($n_\lambda=1$, $n_\mu=1$, $K=0$). The qualitative behavior of the potential curves can also be explained from the well-known behavior of their MO. The $3p\sigma_u$ MO is a promoted orbital and therefore its curve rises steeply at small interelectronic distance (its UA limit is $n=3$). Since it is also pushed up in energy at large electron separation, as in H_2^+, the result is a totally repulsive curve supporting no bound states. The $2p\pi_u$ MO, similarly, first rises in energy for decreasing R, again as in H_2^+. For $R=0$, however, it correlates to $n=2$ and therefore, for decreasing intermediate R, it rapidly decreases in energy. Addition of the interelectronic repulsion and the centrifugal energy dominant as $R\to 0$ results in a potential well, and the long-range behavior gives a small potential barrier such that this curve is responsible for a well-known H^- shape resonance. The $4f\sigma_u$ MO is strongly promoted (UA limit $n=4$) and therefore its energy rises rapidly and much sooner for decreasing R than in the $2p\pi_u$ case. This is the molecular explanation of the different "sizes" of the states of $+$ and $-$ character. The $4f\sigma_u$ is depressed in energy at large R due to the Stark effect and the result is a potential well at intermedi-

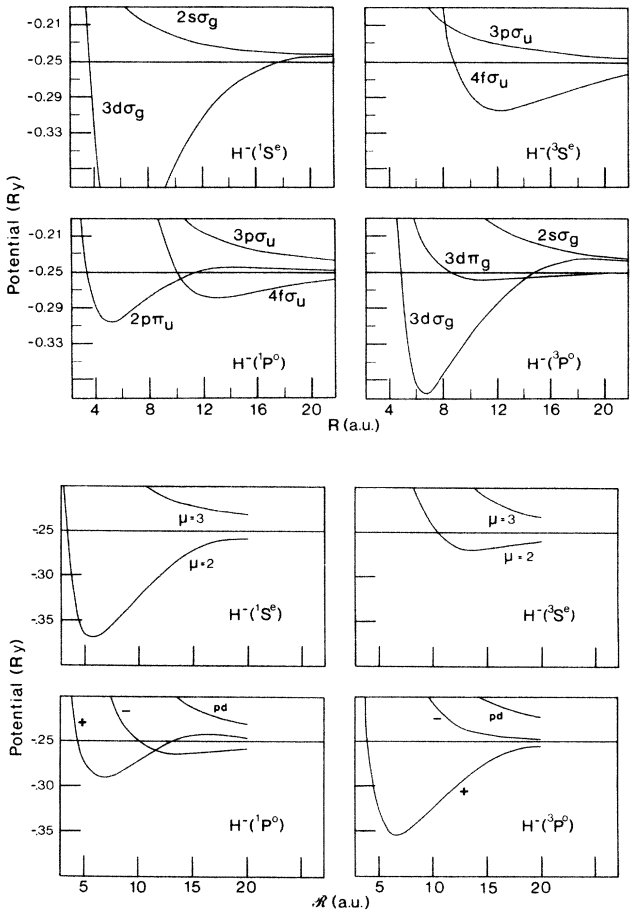

FIG. 3. Potential curves of H^- for states separating to the $N=2$ level of hydrogen. The top four figure parts show MO curves as a function of interelectronic separation R; and the lower four figure parts, hyperspherical curves as a function of hyperradius $\mathcal{R}$ [from Ref. 5(b)].

ate R supporting a series of Feshbach resonances. Similar molecular explanations in terms of electron promotion and long-range Stark behavior can be given of the other potential curves in Fig. 3.

Lin also remarked on the close similarity of the $-$ and *pd* curves of $^1P^o$ symmetry and the curves labeled $\mu=2$ and $\mu=3$ of $^3S^e$ symmetry, although without explanation. The explanation is found here, in that they are pairs of curves built upon the *same pair* of MO's, namely, the $4f\sigma_u$ and $3p\sigma_u$. The only difference is the extra unit of total angular momentum giving rise to an additional repulsive centrifugal term in the $^1P^o$ case.

The curves of $^3P^o$ symmetry, labeled $+$, $-$, and *pd* by Lin are seen to be clearly identified with the *gerade* counterparts of $2p\pi_u$, $4f\sigma_u$, and $3p\sigma_u$, namely, the $3d\pi_g$, $3d\sigma_g$, and $2s\sigma_g$ MO's. However, the MO curves exhibit real crossings, which appear as avoided crossings in the hyperspherical case. In fact, in the $^1P^o$ case, an avoided crossing between $+$ and $-$ curves is traditionally drawn through in the hyperspherical literature, as is done in Lin's curve shown in Fig. 3. This diabatic connection is made since the avoidance of the crossing is small and the connection is necessary to preserve the interpretation of the resonance structure. From the MO results, one sees that the underlying symmetry causing the narrow avoided crossing in Lin's calculation is the validity of the K quantum number (T in Lin's notation). In our case, the two MO's are of σ and π symmetry and cross exactly. The off-diagonal rotational coupling will cause the MO crossing to be avoided. Completely equivalent remarks apply to the crossings seen in our $^3P^o$ and $^3S^e$ curves, compared to the absence of such crossings in Lin's curves. As Starace and Macek[36] have pointed out, it will be necessary to diagonalize the rotational coupling in a MO basis at large R where states of different K become near-degenerate. Nevertheless, it appears that at intermediate R, as clearly demonstrated in the $^1P^o$ case, the MO symmetries provide a more meaningful zeroth-order adiabatic basis.

The MO potential curves of H_2^+ have also been scaled to the case of helium, and a sample is shown in Fig. 4 in comparison with adiabatic hyperspherical curves of Macek.[4] The similarities (we show only states separating to the $N=2$ level) are again clear, but the influence of avoided crossings is more marked. The $2p\pi_u$ MO again provides the deep well of the $^1P^o$ state of $+$ character, but the hyperspherical calculation shows a narrow avoidance with the $-$ level. This avoidance has again been drawn through ($^1P^o$ curves 1 and 2 in Fig. 4) as in H^- (Fig. 3). Klar and Klar's calculation,[6] however, shows a strong avoided crossing between these two states. Again the $2p\pi_u$ and $4f\sigma_u$ MO curves cross. The increased binding resulting from the increased nuclear charge in helium compared with H^- causes the promoted $3p\sigma_u$ MO to exhibit a shallow minimum (it is entirely repulsive in H^-) and to cross with the $3p\sigma_u$ MO around $R=4$ a.u. These two MO's couple via a radial coupling and the corresponding hyperspherical curves show a strong avoidance.

Finally, we have scaled the H_2^+ MO curves to obtain adiabatic potential curves for the system Ps^-. The $^1P^o$

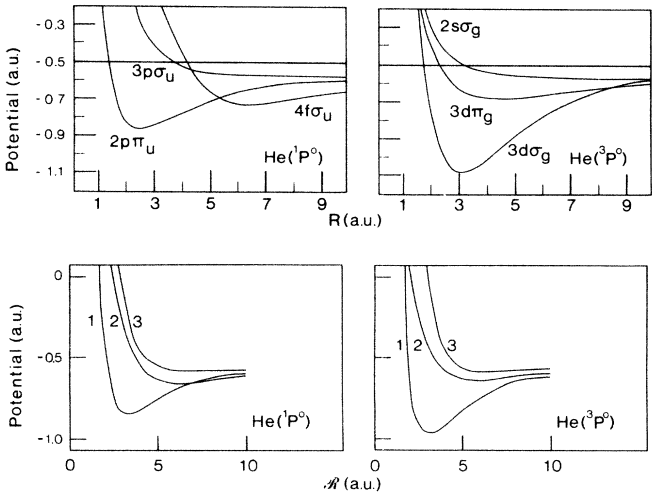

FIG. 4. Potential curves of He for states separating to the $N=2$ level of the He^+ ion. The top two figure parts show MO curves as a function of interelectronic separation R; and the lower two figure parts, hyperspherical curves as a function of hyperradius $\mathcal{R}$ (from Ref. 4).

curves shown in Fig. 5 in comparison with those of Botero and Greene[8] as a function of hyperradius

$$\mathcal{R}=(\mu_{12}R^2+\mu_{12,3}r^2)^{1/2}$$

are, as one expects from the scaling property, very similar to the corresponding curves in H^-. The lower reduced mass $\mu_{12,3}$ of the MO r-coordinate motion is principally responsible for the increased size relative to H^-. Again one should note that the crossing between the + and − curves was simply drawn through by Botero and Greene on the assumption of diabatic hyperspherical behavior. Once more we interpret this as a manifestation of adiabatic MO behavior.

IV. OFF-DIAGONAL COUPLINGS AND TRANSITION OPERATORS

The adiabatic MO's provide a zeroth-order description of the states of two-electron atoms in which the fundamental symmetries of internal electronic motion are described. This model allows one to estimate bound-state and resonant-state positions by solving for the vibrational-state energies in the potential curves of Figs. 3–5. However, to obtain accuracy in the location of energy levels or to discuss dynamical processes such as autoionization or light emission and absorption, it is clear that off-diagonal, symmetry-breaking dynamical couplings must be taken into account. This can be achieved by solving not for single-channel vibrational energies, but by directly solving the set of coupled equations (2.9). We will discuss the consequences of this procedure in the

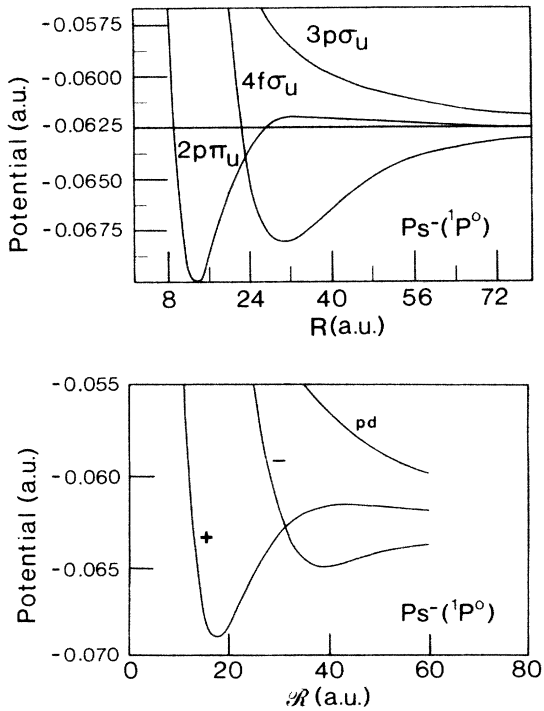

FIG. 5. Potential curves of Ps^- for states separating to the $N=2$ level of positronium. The upper figure part shows MO curves as a function of interelectronic separation R; and the lower figure part, hyperspherical curves as a function of hyperradius $\mathcal{R}$ (from Ref. 8).

case of the MO's separating to the $N=2$ and $N=1$ SA limits. We will then discuss how photoemission and absorption are described in the MO model.

In the adiabatic potential energy curves leading to the $N=2$ manifold, discrete states are stationary. However, since they lie in the $N=1$ continuum, they will autoionize. In the single-particle picture of two-electron atoms, this autoionization is caused by the residual electron-electron potential interaction that is not diagonalized by the single-particle basis (e.g., Hartree-Fock). In our MO model, however, the full electron-electron plus electron-nucleus interactions are diagonalized by the MO basis. Hence it is the *dynamical* couplings, neglected by the assumption of a rigid interelectronic molecular axis, that give rise to the decay of states lying energetically above the first ionization threshold. Such bound vibrational states in a SA $N=2$ MO undergo a transition to an isoenergetic vibrationally unbound state of an $N=1$ MO. This results in ejection of the electron as the MO separates to the $N=1$ one-electron ground state. The width of the autoionizing states depends not only upon the magnitude of the MO coupling but also upon the overlap of the vibrational bound and unbound wave functions. In the single-particle description, the width is proportional to the (suitably antisymmetrized) two-electron matrix element

$$\langle \phi_{1s}(\mathbf{r}_1)\phi_\epsilon(\mathbf{r}_2) \mid e^2/r_{12} \mid \phi_{Nlm}(\mathbf{r}_1)\phi_{N'l'm'}(\mathbf{r}_2)\rangle \ . \tag{4.1}$$

Since the operator is scalar, the only selection rules are the conservation of the total state quantum numbers $LS\pi$. This is, of course, still required in the MO picture, but the identification of approximate internal symmetries leads to corresponding approximate selection rules for the autoionizing decay.

The principal selection rule is that the g,u MO symmetry is strictly preserved. The second selection rule arises from the requirement that radial coupling matrix elements involving the $\partial/\partial R$ operator have $\Delta K=0$ and rotational coupling elements with the $l_\pm$ transition operator have $\Delta K=\pm 1$ only. Pictorially, these operators correspond for radial coupling to a squeezing or stretching of the interelectronic axis which changes the λ,μ nodal structure of the electronic c.m. motion with respect to the nucleus, without changing its alignment with respect to the molecular axis (hence $\Delta K=0$). For rotational coupling, the electronic c.m. motion changes its alignment with respect to the molecular axis due to a rapid rotation of that axis which the electronic c.m. cannot follow. These are the two dynamical effects leading to decay of high-lying states. The selection rules are summarized in Table I.

The $1s\sigma_g$ and $2p\sigma_u$ MO's separating to $N=1$ support excited states which do not decay (only in the case of helium does the $2p\sigma_u$ antibonding MO support bound states). However, their *energies* will be shifted by the dynamical interactions. For example, the $1s\sigma_g$ (which supports the $^1S^e$ ground state) will mix with the $2s\sigma_g$ and $3d\sigma_g$ by radial coupling in the $^1S^e$, $^3P^o$, $^1D^e$, etc., series and with the $3d\pi_g$ by rotational coupling in the $^3P^o$, $^1D^e$, etc., series. By contrast, the $2p\sigma_u$ MO (which supports the lowest triplet S state) mixes radially with the $3p\sigma_u$

TABLE I. The states of $L=0$ and 1 symmetry built on the MO separating to the $N=1$ and 2 levels and the off-diagonal couplings between them. Dashes denote null values.

Stark (n_1n_2m)	(000)		(100)		(010)		(001)	
MO $(n_\lambda n_\mu K)$	$1s\sigma_g$	$2p\sigma_u$	$2s\sigma_g$	$3p\sigma_u$	$3d\sigma_g$	$4f\sigma_u$	$3d\pi_g$	$2p\pi_u$
$1s\sigma_g$ (000)	$^1S^e, ^3P^o$	–	Rad.	–	Rad.	–	Rot. $^3P^o$	–
$2p\sigma_u$ (010)		$^3S^e, ^1P^o$	–	Rad.	–	Rad.	–	Rot. $^1P^o$
$2s\sigma_g$ (100)			$^1S^e, ^3P^o$	–	Rad.	–	Rot. $^3P^o$	–
$3p\sigma_u$ (110)				$^3S^e, ^1P^o$	–	Rad.	–	Rot. $^1P^o$
$3d\sigma_g$ (020)					$^1S^e, ^3P^o$	–	Rot. $^3P^o$	–
$4f\sigma_u$ (030)						$^3S^e, ^1P^o$	–	Rot. $^1P^o$
$3d\pi_g$ (011)							$^1P^e, ^3P^o$	–
$2p\pi_u$ (001)								$^1P^o, ^3P^e$

and $4f\sigma_u$ and rotationally with the $2p\pi_u$. Conversely, the same selection rules govern the decay of the autoionizing states. For example, the $^3P^o$ series built upon $3d\sigma_g$ can only autoionize to a $^3P^o$ state of $1s\sigma_g$ by radial coupling, but the $4f\sigma_u$ $^1P^o$ states will autoionize (also by radial coupling) to a $2p\sigma_u$ $^1P^o$ unbound state. By contrast, the $2p\pi_u$ $^1P^o$ levels (often called the + series in helium) decays by coupling *rotationally* with the $2p\sigma_u$ $^1P^o$ continuum levels. One should mentioned, of course, that the $2p\pi_u$ and $4f\sigma_u$ $^1P^o$ levels will mix among themselves by rotational coupling.

The widths of the autoionizing states will be proportional to such coupling elements. For radial coupling, they are diagonal in $LS\pi$ and t and also in K. They have the form

$$\delta_{KK'}\int dR\, f_{iK}(R)\langle\phi_{iK}\mid\partial/\partial R\mid\phi_{jK'}\rangle\frac{\partial f_{jK'}}{\partial R}\ . \tag{4.2}$$

For rotational coupling, they are also diagonal in $LS\pi$ and t, but have $\Delta K=\pm1$ and are of the form

$$\lambda_\pm\int dR\, f_{iK}(R)\langle\phi_{iK}\mid l_\pm\mid\phi_{jK\pm1}(R)\rangle f_{jK\pm1}(R)\ . \tag{4.3}$$

In both cases, if the MO matrix element varies relatively slowly with R, then it may be removed from the R integral at the upper-state equilibrium separation R. Then a factor remains depending essentially upon the overlap of the two vibrational wave functions, bound and continuum, for initial and final states, respectively, in the case of autoionization.

The states may also decay by photon emission. Here the selection rules are very different, although, as is shown below, the transition matrix element assumes a very transparent form in the MO description. The interaction with the radiation field can be described by an operator $\mathrm{Re}(Ee^{-i\omega t}\mathbf{e}_\beta\cdot\boldsymbol{\rho})$, where E is the field strength at frequency ω, $\mathbf{e}_\beta$ is the (complex) polarization vector of the light and $\boldsymbol{\rho}$ is the atomic dipole operator. The matrix element of relevance is

$$\langle\Psi_{LM\pi}\mid\mathbf{e}_\beta\cdot\boldsymbol{\rho}\mid\Psi_{L'M'\pi'}\rangle$$

for transition from an initial state $\Psi_{L'M'\pi'}$ to a final state $\Psi_{LM\pi}$ [from Eq. (2.13)]. In LS coupling, the spin quantum number is conserved. In the laboratory fixed frame, in atomic units,

$$\mathbf{e}_\beta\cdot\boldsymbol{\rho}=\mathbf{e}_\beta\cdot(\mathbf{r}_1+\mathbf{r}_2)=2\mathbf{e}_\beta\cdot\mathbf{r}\ , \tag{4.4}$$

where r is the position of the two-electron c.m. with respect to the nucleus. Equations (4.4) demonstrate the convenient result that the total dipole moment operator of the two-electron atom is *independent* of the adiabatic coordinate $\mathbf{R}$. This separation is to be contrasted with the hyperspherical treatment where the dipole operator $(\mathbf{r}_1+\mathbf{r}_2)$ mixes "internal" coordinates and the adiabatic hyperspherical radius $\mathcal{R}$. The formula (4.4) is also interesting in that, apart from the factor 2, it is identical with the dipole operator for the absorption of light by an electron in the H_2^+ molecular ion. Hence the familiar language of molecular spectroscopy can be used. With (2.13) and (4.4), the dipole matrix element can be written formally as

$$\langle \Psi_{LM\pi} \mid \mathbf{e}_\beta \cdot \boldsymbol{\rho} \mid \Psi_{L'M'\pi'} \rangle = \int dR\, f_{iK}(R) f_{iK'}(R) \langle \phi_{iK} \mid (2\mathbf{e}_\beta \cdot \mathbf{r})_{BF} \mid \phi_{iK'} \rangle \ , \tag{4.5}$$

where the dipole operator has been transformed to the body-fixed frame and the angular integral over $\hat{\mathbf{R}}$ performed. By standard means, one obtains Clebsch-Gordon coefficients resulting in the well-known molecular selection rules $q'+M'=M$, $q+K'=K$. The latter leads to the condition that in the MO dipole integral in (4.6) only $\sigma \leftrightarrow \sigma$, $\pi \leftrightarrow \pi$, etc. transitions are allowed for $q=0$ and only $\sigma \leftrightarrow \pi$, $\pi \leftrightarrow \delta$, etc. for $q=1$. There is a further condition on the MO, arising from the fact that total parity must change but spin is conserved in the dipole transition. Then $\pi\pi'=-1$ but, since $\pi(-1)^S=(-1)^l$ where l is the UA orbital quantum number, we have $\pi\pi'=(-1)^{S+S'+l+l'}=(-1)^{l+l'}$. Hence the two MO's involved must have different UA parity, or what is equivalent, different *gerade-ungerade* symmetry. An example in helium is the dipole allowed ${}^1S^e \rightarrow {}^1P^o$ transitions from the ground state (lowest vibrational state of $1s\sigma_g$, $L=0$ potential) to the $(1snp)$-like series (vibrational levels of the $2p\sigma_u$, $L=1$ potential). In this case, if the matrix element

$$\langle 2p\sigma_u \mid (\mathbf{e}_\beta \cdot \mathbf{r})_{BF} \mid 1s\sigma_g \rangle$$

is a slowly-varying function of R then it may be brought out of the integral and the relative strength of absorption $(1s^2)\ {}^1S^e \rightarrow (1snp)\ {}^1P^o$ would be described in the MO model by the square of the Franck-Condon integrals

$$I_n = \int dR\, f^{(n)}_{2p\sigma_u}(R) f^{(0)}_{1s\sigma_g}(R) \ . \tag{4.6}$$

Thus one sees that the language of molecular spectroscopy finds complete application in the MO description of atomic spectroscopy. Such an analysis helps to explain, for example, why the $1s\sigma_g \rightarrow 2p\pi_u$ absorption to the ${}^1P^o$ + series in helium is much stronger than the $1s\sigma_g \rightarrow 4f\sigma_u\ {}^1P^o$ − series. The potential minimum of the $4f\sigma_u\ {}^1P^o$ curve (see Fig. 4) lies much farther out than that of the $2p\pi_u$ and hence the Franck-Condon factors with the $1s\sigma_g\ {}^1S^e$ ground vibrational state $(1s^2)$ are much reduced.

V. CONCLUSIONS

We have extended the method of Hunter and coworkers,[19,20] in which the three-body Coulomb problem is treated in molecular $\mathbf{r},\mathbf{R}$ Jacobi coordinates, to the study of states separating to the $N=2$ hydrogenic manifold in He, H^-, and Ps^-. Adiabatic potential curves for these systems are obtained by scaling the corresponding potential curves for the H_2^+ molecular ion. The scaling procedure gives MO potential curves in close correspondence with adiabatic potential curves resulting from a separation in hyperspherical coordinates. Thereby the MO scaling property accounts indirectly for the similarity between hyperspherical potentials for He, H^-, and Ps^-. The potential curves have unique quantum numbers n_λ, n_μ, and K, which correlate to the UA spherical quantum numbers n,l,m and the SA parabolic quantum numbers n_1,n_2,m. The conservation of the associated nodal surfaces for all interelectronic separations explains the "almost-good" quantum numbers K_H, A, and T associated with hyperspherical potential curves. These latter quantum numbers are in one-to-one correspondence with MO quantum numbers and can be replaced by them. In particular, the quantum number T is identical to the familiar σ, π, δ etc. labeling of MO, corresponding to angular momentum projection $K=0$, 1, 2, etc. The quantum number A is given by $(-1)^{n_\mu}=(-1)^{l-K}$, where n_μ gives the number of hyperbolic nodal surfaces (where $r_1=r_2$). The quantum number K_H of Herrick is found to be simply the value of (n_2-n_1) for the separated-atom Stark level to which the MO correlates. It is also the eigenvalue of a_z, the z component of the SA Runge-Lenz vector. Alternatively, K_H can be identified as the asymptotic eigenvalue of the two-center operator $\Omega(R)$ arising from the separation of the MO problem in λ,μ coordinates. Finally, attention has been drawn to the validity of the MO quantum number $(-1)^l=(-1)^t=\pi(-1)^S$ for overall two-electron states. This corresponds to states being of even (g) or odd (u) symmetry under reversal of the internal MO coordinate $\mathbf{r}$. Its presence accounts for the occurrence of sequences of states of similar character, e.g., ${}^1S^e$, ${}^3P^o$, ${}^1D^e$, etc. which arise from all MO's of σ_g symmetry. Previously, such sequences have been identified only on the basis of complicated group-theoretical arguments.

In the MO model, the process of autoionization is analogous to the dissociation of molecules, e.g., $H_2^+ \rightarrow H^+ + H$, and selection rules allow one to identify decay modes due to either radial or rotational coupling in the MO basis. The process of light absorption is particularly simple, since the electromagnetic field couples only to the MO coordinate $\mathbf{r}$. Again, this is in complete analogy to the description of vibronic transitions in molecules arising from the absorption of light.

ACKNOWLEDGMENTS

We would like to express our gratitude to P. T. Greenland for helpful consultation on the subject of nodal surfaces in the two-center Coulomb problem. This work was partially supported by the Deutsche Forschungsgemienschaft under the Schwerpunktprogramm Atom- und Molekültheorie and by the U.S. Department of Energy (Division of Chemical Sciences, Offices of Basic Energy Sciences and Energy Research).

[1]U. Fano, Rep. Prog. Phys. **46**, 97 (1983).
[2]L. Lipsky, R. Anania, and M. J. Conneely, At. Data Nucl. Data Tables **20**, 127 (1977).
[3]J. W. Cooper, U. Fano, and F. Prats, Phys. Rev. Lett. **10**, 518 (1963).
[4]J. Macek, J. Phys. B **1**, 831 (1968).
[5](a) C. D. Lin, Phys. Rev. A **10**, 1986 (1974); (b) **16**, 30 (1976); (c) **25**, 76 (1982); (d) **29**, 1019 (1984).

[6]H. Klar and M. Klar, J. Phys. B **13**, 1057 (1980).
[7]J. E. Hornos, S. W. MacDowell, and C. D. Caldwell, Phys. Rev. A **33**, 2212 (1986).
[8]J. Botero and C. H. Greene, Phys. Rev. Lett. **56**, 1366 (1986).
[9]D. R. Herrick, M. E. Kellman, and R. D. Poliak, Phys. Rev. A **22**, 1517 (1980).
[10]M. E. Kellman and D. R. Herrick, Phys. Rev. A **22**, 1536 (1980); J. Phys. B **11**, L755 (1978).
[11]D. R. Herrick, Adv. Chem. Phys. **52**, 1 (1983).
[12]D. R. Herrick and M. E. Kellman, Phys. Rev. A **21**, 418 (1980).
[13](a) J. M. Feagin, J. Phys. B **17**, 2433 (1984); (b) Bull. Am. Phys. Soc. **29**, 801 (1984); (c) Nucl. Instrum. Methods **B24/25**, 261 (1987).
[14](a) J. M. Feagin, J. S. Briggs, and T. Weissert, in *Abstracts of the Fourteenth International Conference on the Physics of Electronic and Atomic Collisions, Palo Alto, CA, 1985,* edited by M. J. Coggiola, D. L. Huestis, and R. P. Saxon (ICPEAC, Palo Alto, 1985), p. 147. (b) J. M. Feagin and J. S. Briggs, Phys. Rev. Lett. **57**, 984 (1986).
[15]H. J. Yuh, G. S. Ezra, P. Rehmus, and R. S. Berry, Phys. Rev. Lett. **47**, 497 (1981).
[16]G. S. Ezra and R. S. Berry, Phys. Rev. A **28**, 1974 (1983).
[17]J. L. Krause, J. D. Morgan, and R. S. Berry, Phys. Rev. A **35**, 3189 (1987).
[18]S. Watanabe and C. D. Lin, Phys. Rev. A **34**, 823 (1986).
[19]G. Hunter, B. F. Gray, and H. O. Pritchard, J. Chem. Phys. **45**, 3806 (1966).
[20]G. Hunter and H. O. Pritchard, J. Chem. Phys. **46**, 2146 (1967); **46**, 2153 (1967).
[21]J. Maddox, Nature **323**, 391 (1986).
[22]R. T. Pack, Phys. Rev. A **32**, 2022 (1985).
[23]H. Essén, Int. J. Quantum. Chem. **XII**, 721 (1977).
[24]J. M. Rost and J. S. Briggs, Z. Phys. D **5**, 339 (1987).
[25]J. D. Power, Proc. R. Soc. London, Ser. A **274**, 663 (1973).
[26]P. T. Greenland, Phys. Rep. **81**, 131 (1982).
[27]D. R. Bates and R. H. G. Reid, Adv. At. Mol. Phys. **4**, 13 (1968).
[28]D. R. Herrick and O. Sinanoglu, Phys. Rev. A **11**, 97 (1975).
[29]K. Mølmer and K. Taulbjerg, J. Phys. B (to be published).
[30]C. A. Coulson and A. Joseph, Int. J. Quantum. Chem. **1**, 337 (1967).
[31]M. Barat and W. Lichten, Phys. Rev. A **6**, 211 (1972).
[32]J. C. Slater, *Quantum Theory of Matter* (Krieger, Huntington, 1977), Chap. 20.
[33]R. T. Pack and J. O. Hirschfelder, J. Chem. Phys. **52**, 4198 (1970).
[34]A. Fröman, J. Chem. Phys. **36**, 1460 (1962).
[35]C. J. H. Schutte, *The Theory of Molecular Spectroscopy* (North-Holland, Amsterdam, 1976), Vol. I, Chap. 5.
[36]A. F. Starace and J. H. Macek, Phys. Rev. Lett. **58**, 2385 (1987).